Analytical Methods

ROYAL SOCIETY OF CHEMISTRY

PAPER

View Article Online
View Journal | View Issue

Cite this: *Anal. Methods*, 2025, **17**, 3415

Uncovering gunshot residue flow and deposition mechanisms using novel visualization methods, real-time atmospheric particle sampling, and spectrochemical techniques†

Thomas D. Ledergerber, [a] Matthew Staymates, [b] Kourtney A. Dalzell, [c] Luis E. Arroyo, [ac] Roger Jefferys[c] and Tatiana Trejos *[ac]

Gunshot residue (GSR) consists of inorganic and organic components released during firearm discharge. Understanding the generation, transport, and settlement of these residues is essential to assess exposure risks and answer questions of forensic interest. Since GSR is prone to depositing in the vicinity of a firing event, its presence on a person of interest is meaningful to evaluate hypotheses about who discharged a firearm or if GSR was acquired by alternative means such as indirect transfer, being a bystander, or passing through the area shortly thereafter. However, the complexity of GSR production and variable dispersion makes its interpretation challenging. This study employs a novel multi-sensor approach to enhance the current understanding of GSR deposition, transference, and persistence. First, a particle counting/sizing system and inexpensive custom-made atmospheric samplers measure the population of airborne particles before, during, and after the firearm discharge. Second, high-speed videography and laser sheet scattering reveals visual and qualitative information about the flow of GSR under various experimental conditions. Finally, SEM-EDS and LC-MS/MS permit the confirmation of the elemental and chemical makeup of residues. This study estimates (a) how IGSR/OGSR are produced during a firing event using various firearms and ammunition, (b) how long it takes to settle on surfaces located at various distances from the firing location, and (c) direct and indirect deposition in indoor, semi-enclosed, and outdoor environments. The combination of these analytical tools provides breakthrough knowledge in forensics and other disciplines where airborne exposure is central, such as environmental sampling and indoor air quality.

Received 20th December 2024
Accepted 31st March 2025

DOI: 10.1039/d4ay02283a

rsc.li/methods

1 Introduction

The analysis of gunshot residue (GSR) can play a key role in assessing potential environmental exposures and reconstructing the events leading up to a crime.[1,2] While this study focuses on the forensic implications, the findings derived from this study have expanded applicability in public safety.[3–5] Knowledge gained through GSR analysis can uncover important details about the locations and actions of persons of interest who may have been involved in a criminal activity. However, sound studies offering perspective on the mechanisms of GSR production, flow, and deposition are needed to enhance our knowledge regarding the complex dynamics occurring during the discharge of a firearm.

When a firearm is discharged, particles and residues of both inorganic and organic nature are released into the surrounding environment.[1,2,6–8] These are respectively known as inorganic (IGSR) and organic gunshot residue (OGSR). IGSR primarily results from the primer of a cartridge. During the firing event, the firing pin strikes the primer, which contains shock-sensitive components such as lead styphnate, as well as oxidizers and fuels, including barium nitrate and antimony trisulfide.[2] This results in a chain deflagration, which in turn ignites the explosives in the smokeless powder, including nitrocellulose and nitroglycerin, as well as certain stabilizing compounds.[9–11] After the firing process is complete, the plume of hot gas begins to condense, forming both IGSR and OGSR. These particles and residues may settle onto nearby surfaces, allowing forensic analysts to determine that a firearm may have been discharged in a given location. Additionally, these particles and residues may fall onto the hands or clothing of a person(s) of interest and surrounding surfaces, which can assist in developing

[a]*West Virginia University, Department of Chemistry, Morgantown, WV 26506, USA. E-mail: tatiana.trejos@mail.wvu.edu*

[b]*National Institute of Standards and Technology, 100 Bureau Dr, Gaithersburg, MD 20899, USA*

[c]*West Virginia University, Department of Forensic and Investigative Science, Morgantown, WV 26506, USA*

† Electronic supplementary information (ESI) available. See DOI: https://doi.org/10.1039/d4ay02283a

investigative leads and reconstructing events.[1,12,13] The complexity of interpreting GSR evidence, however, lies in the fact that GSR can also be deposited on other individuals located either at the scene or outside of the scene by direct or indirect transfer.

The current standard practice for GSR analysis involves scanning electron microscopy-energy dispersive X-ray spectrometry (SEM-EDS).[14] This technique is used to determine the size, morphology, and elemental composition of individual IGSR particles following ASTM E1588-20.[14] While this technique is very effective for the identification of IGSR, it is limited in its ability to produce relevant case information about the events leading up to a crime (such as the reliable identification of the individual that discharged a firearm when multiple persons are present) when used as a standalone method.

To complement current standard practice, recent studies have detailed the analysis of OGSR.[2,9,15–18] Traditionally, liquid chromatography-tandem mass spectrometry (LC-MS/MS) and gas chromatography-mass spectrometry (GC-MS) have been used to detect explosives and stabilizers present in OGSR.[2,9,12,13,19] More recently, faster methods, including electrochemistry, Raman spectroscopy, and ambient ionization-mass spectrometry methods, have been applied to the analysis of organic components.[17,20–23] While these methods alone may be insufficient for confirmation of GSR, the orthogonal information of IGSR and OGSR can enhance the quality of information obtained from a piece of evidence.

Traditional analytical techniques offer valuable chemical information, but methods for real-time GSR flow patterns and distribution analysis are still needed to understand the relevance of the evidence within the context of the transfer and deposition mechanisms. A study published in 2021 by Luten *et al.* detailed the novel application of real-time atmospheric sampling to the analysis of airborne GSR.[24] In this study, they used a particle counter and air impactor to count and size airborne GSR following a firing event. The authors determined that airborne GSR may persist for several hours following the firing event. Additionally, they found that there is a risk of contamination by IGSR for up to three hours following a discharge.

A study in 2011 by Gerard *et al.* investigated the deposition of GSR across distances ranging from 0 m to 18 m downrange from the firearm through SEM-EDS analysis.[25] Key findings included that GSR particles tend to travel along the path of the projectile with the highest concentration of particles depositing approximately 13.5 m downrange. It was determined that the concentration of IGSR particles cannot be used alone to distinguish between a shooter and any other involved individuals, such as a bystander. Another study in 2011 by Lindsay *et al.* evaluated IGSR exposure between a shooter and bystander.[26] Shooters and bystanders were sampled for IGSR 15 minutes after exposure. The authors found that bystanders sometimes had similar concentrations of IGSR recovered from hands, making differentiation *via* particle counts not viable. These studies have laid the groundwork for the hypothesis that it is not possible to determine the identity of a shooter or bystander through GSR analysis. Therefore, further studies into examining the potential for the differentiation of a shooter, bystander, or passerby are crucial to the field of forensic science. The ability to determine with reasonable confidence not only that an individual has GSR present on them, but rather if the person fired a gun offers immense evidentiary value.

In this study, we present a novel approach using several complementary methods for the analysis of gunshot residue, measuring both IGSR and OGSR, to better understand the flow of GSR in an enclosed room and the possible implications this can have on the classification of individuals involved in or simply in contact with a crime scene. First, we employ two atmospheric particle counting methods. These include a series of nine customized particle counters traditionally used in environmental atmospheric sampling.[27–31] For comparison, a more robust particle counting and sizing system is used. To complement these methods, both LC-MS/MS and SEM-EDS are used as confirmatory methods for the determination of the GSR deposition processes. Finally, both high and low-speed videography combined with laser sheet scattering are used to offer insightful and novel visual information about the flow of GSR in scenarios involving different firearms, varying numbers of shots, the interactions between GSR and a bystander, and the effects of airflow in enclosed and open spaces. This unique combination of multiple sensors and data from both inorganic and organic GSR is reported for the first time, discovering similarities and differences in the creation of IGSR and OGSR, and their interaction with persons and objects in the vicinity of the firing.

This study aims to provide a fundamental understanding that can inform evaluations of the presence and interpretation of GSR. There have been many recent studies on the transfer of GSR. However, these studies primarily focus on the secondary or tertiary transfer of GSR from one individual to another or from a surface to an individual.[10,11,32] Here, we investigate the primary transfer of GSR from the firearm to multiple individuals in shooter, bystander, and passerby scenarios. Additionally, in this study, we evaluate the persistence of GSR suspension in the air surrounding a firing event to provide information regarding an individual's exposure to GSR without coming into contact with another person or surface.

2 Materials and methods

2.1. Overview of the multi-method approach

This study used a multi-method approach that includes the simultaneous visualization of IGSR and OGSR using laser sheet scattering and videography, and the measurement of particle size and distributions using particle samplers. Additionally, analysis of the IGSR by SEM-EDS and OGSR by LC-MS/MS was conducted on various static and dynamic collection devices. Together, the analytical data was analyzed to reveal mechanisms of production, flow, and deposition of IGSR and OGSR residue. Fig. 1 summarizes the main techniques and information investigated in this study while briefly describing some of the main questions of interest. The following sections provide detailed information on the experimental designs and instrumentation utilized.

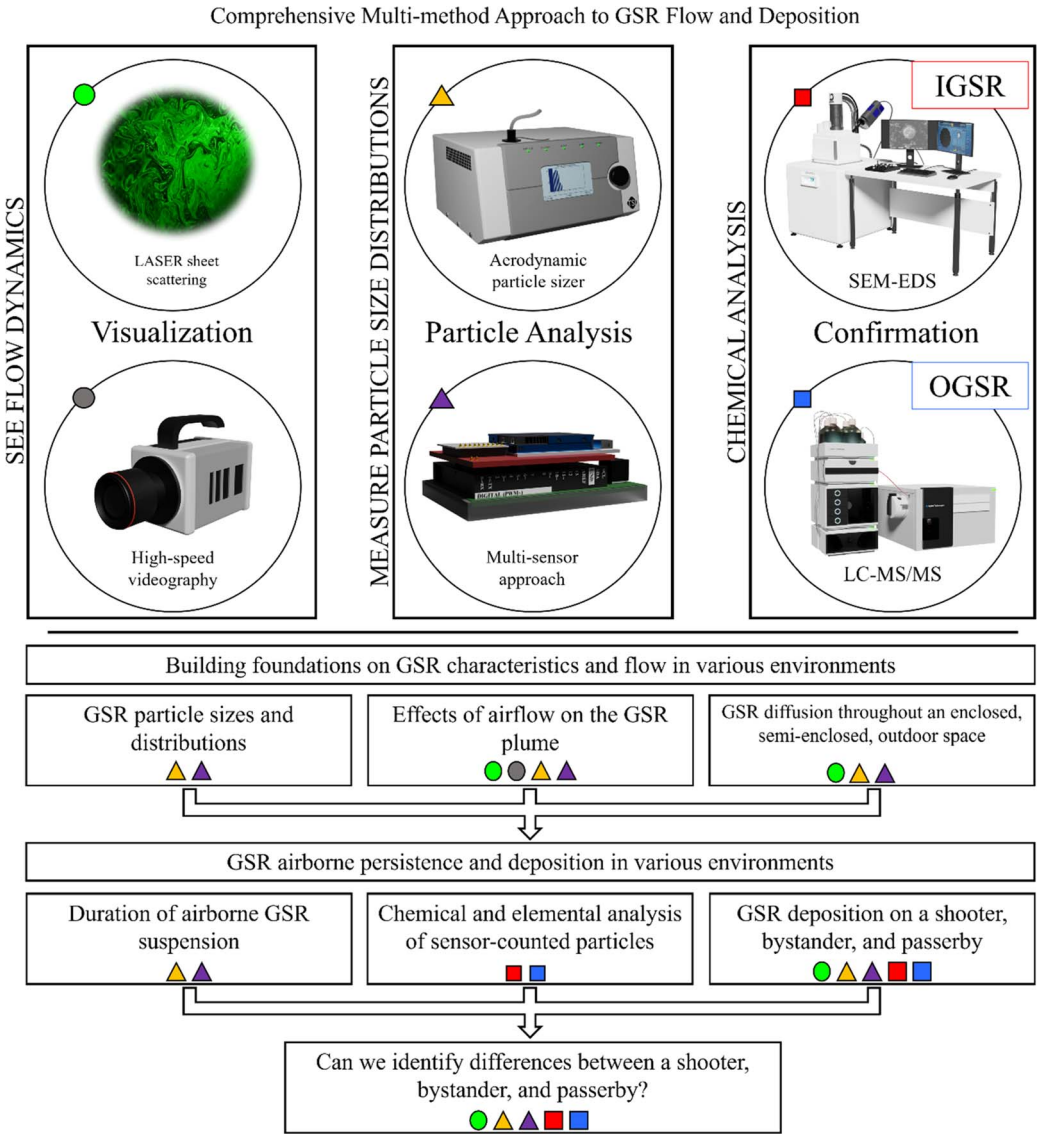

Fig. 1 Layout of experimental techniques used in this study separated by the type of information they offer. Techniques are coded with a colored shape, indicating the sections of the study in which they were used. Green and gray circles represent laser scattering and high-speed videography for visualization of GSR, and yellow and purple triangles represent particle analyses by APS or PCs, respectively. The red and blue squares represent the SEM-EDS and LC-MS/MS, respectively.

2.2. Overview of the experimental design

The multi-method approach was used to evaluate the characteristics of GSR flow and deposition under the effect of different independent variables. The experiments collected data from 958 samples over 106 trials. The samples included those measured by particle analysis methods and those collected for subsequent SEM-EDS and LC-MS/MS analysis. Several of these experiments were complemented with videography to visualize the GSR flow dynamics. A detailed summary of the experimental setup is shown in Fig. 2, with the respective dependent and independent variables, number of trials, and number of samples per trial.

The first experiments were performed to evaluate the overall behavior of airborne GSR under various shooting and environmental conditions. All measurements were done using the APS and the particle counter systems and visualized with the laser scattering videos (see Fig. 2, experiments A1 to A3). The effects of firearm/ammunition types (up to seven types) and environmental conditions (outdoor/indoor) on the resultant GSR's particle sizes and distributions produced were measured (Fig. 2A1). Second, the effect of the shooting range ventilation system on GSR flow dynamics was evaluated, and the findings were utilized to develop protocols to prevent carry-over between trials (Fig. 2A2). Finally, the effects of altered environmental conditions (outdoor, indoor, and semi-enclosed vehicles) on the diffusion and spread of GSR were evaluated at different locations relative to the shooting site (at the shooter's site, 4 m away, and outside and inside the vehicle, Fig. 2A3). The second experiment evaluated the effect of environmental conditions on the duration of airborne suspension of GSR. Here, the firearm

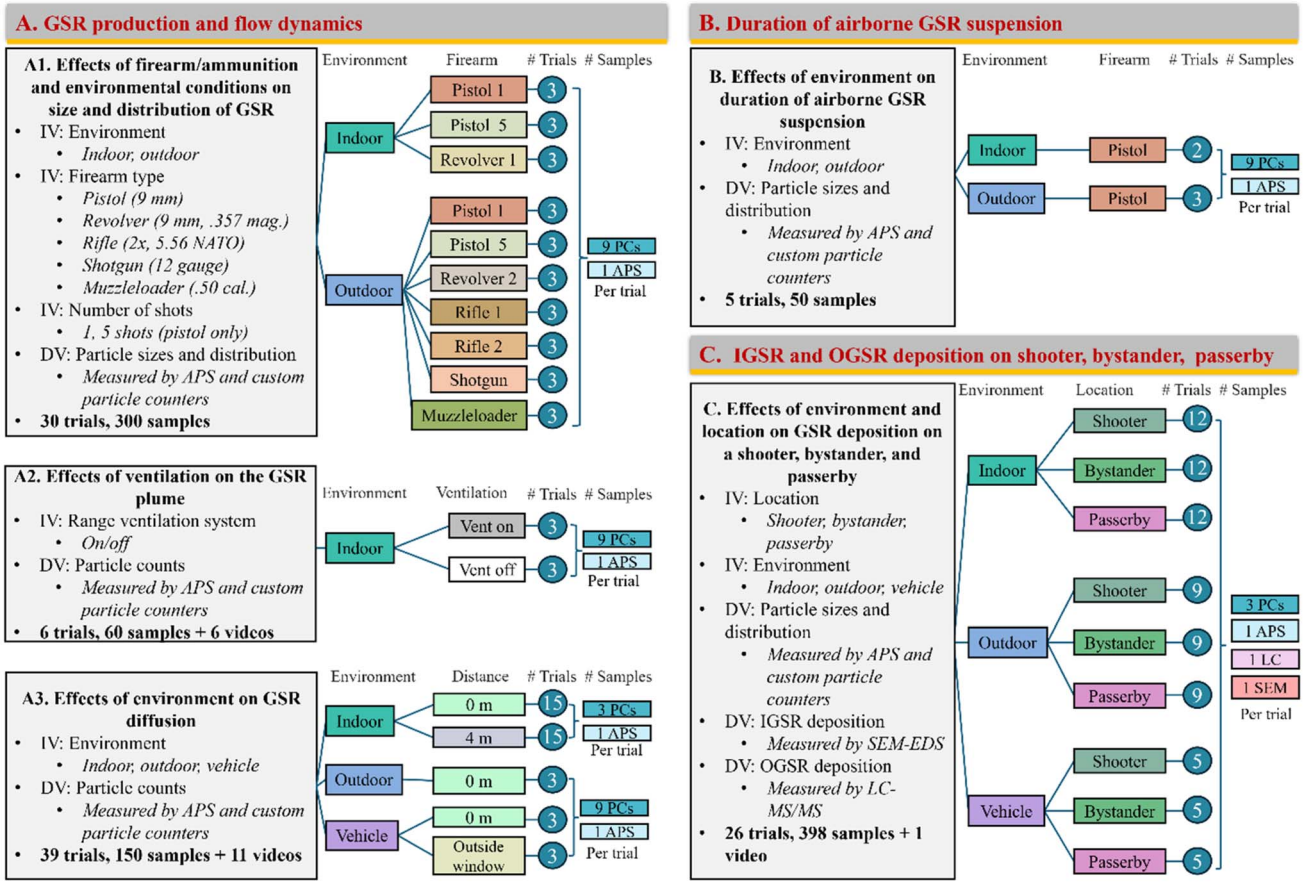

Fig. 2 Diagram of the experimental setup of this study. Three main experiments were conducted. First, the GSR production and flow dynamics (A) were studied under various environmental and shooting conditions. Second, the effect of the environment on the duration of airborne suspension was evaluated (B). Finally, the effects of the environment and relative location to individuals on the GSR particle size, distribution, and deposition were evaluated (C). Each experiment's topic of interest is provided in bold lettering (A–C) with the respective independent and dependent variables listed. Randomized blocked experimental designs were used, showing the factors/groups, the respective number of trials, and samples collected per trial and analytical method. Legends: IV: independent variable, DV: dependent variable; environment (indoor, outdoor, vehicle), firearm (pistol 9 mm fired once, pistol 1, or 5 times, pistol 5; revolver 9 mm, revolver 1, or .357 magnum, revolver 2; rifle 2×, rifle 1 or 5.56 NATO, rifle 2; shotgun 12 gauge, and muzzleloader .50 caliber); and methods (APS: aerodynamic particle sizer, PCs: particle counters, LC: LC-MS/MS, and SEM: SEM-EDS).

and ammunition were kept constant (pistol 9 mm), and the deposition times were estimated from measurements from the APS and PC systems (Fig. 2B). Finally, the third experiment evaluated the effects of environmental conditions and location relative to the firearm (shooter, bystander, and passerby) on the deposition of the individuals of interest. This study used a comprehensive multi-method approach, including atmospheric sampling methods, visualization laser scattering methods, and analytical techniques to analyze IGSR and OGSR (Fig. 2C). More detailed explanations of the experimental setups can be found in Section 2.5 and relevant subsections.

2.3. Instrumentation used in this study

2.3.1. Particle counting/sizing methodology. An APS 3321 aerodynamic particle sizer (TSI Incorporated, Shoreview, MN, USA), operating at an airflow rate of 5 L min^{-1}, was used to provide information regarding counts and size distributions of airborne GSR. The APS operates by measuring light scattering intensity aerodynamic time of flight of particles. This allows for high-resolution measurements of particles ranging from 0.523 μm to 20 μm. Particle counts and distributions were recorded at 10-s and 60-s intervals. Information was collected using Aerosol Instrument Manager (AIM, TSI Incorporated). Data was extracted as an ASCII file and converted to a .xlsx file for processing.

Custom-made particle counters (Fig. S1†) were built from a model PMSA003 (Plantower Technology, Jiangxi Provence, China) atmospheric sampler. Each was attached to an Arduino microcontroller (Arduino, MA, USA) to allow for wireless communication with a computer. Particle counters of this nature have the advantage of being very low cost (~$13 per counter) when compared to instrumentation typically used to measure GSR. This advantage allowed for up to nine particle counters to be deployed simultaneously, adding the ability to measure airborne GSR concentrations in replicates and in various locations of interest. The particle counters use laser

scattering intensity measurements to determine the size of airborne particulates. While this enables them to measure a wide range of particle sizes (0.3–10 μm), the particle counters are more prone to increased uncertainty when sizing irregularly shaped particles. Therefore, the custom-made particle counters were used primarily to determine concentrations of GSR relative to one another.[33] Particle counting information was recorded using LabView 2017 (National Instruments, Texas, USA). Data was translated from a .tdms file using Microsoft Excel.

2.3.2. Visualization of GSR by laser sheet scattering. A laser sheet was created by attaching a cylindrical glass element in front of a green (512 nm, 3 W) laser. This served to spread the beam into a two-dimensional wall of green laser illumination, which can be positioned in any orientation to illuminate a thin (approximately two mm) slice of the area. In combination with a dark room, this allows for the visualization of air-suspended micron-sized particles.[34,35] A high-speed camera, Photron Fastcam NOVA-S9 (Photron, Tokyo, Japan), was used to record grayscale video at 3000 frames per second. Additionally, a Nikon D780 (Nikon, Tokyo, Japan) camera was used to record high-definition, lower framerate (60 frames per second, ISO 2000, aperture F5/5.6, exposure 1/125) video with color.

2.3.3. Chemical and elemental analysis of GSR

2.3.3.1. LC-MS/MS instrumental analysis. Six organic compounds commonly found in GSR were monitored in this study using previously reported instrumental parameters.[6,15–17] These included Akardite II (AKII), diphenylamine (DPA), ethyl centralite (EC), methyl centralite (MC), 2-nitrodiphenylamine (2-NDPA), and 4-nitrodiphenylamine (4-NDPA). Deuterated diphenylamine (D_{10}-DPA) was used as an internal standard. An Agilent 1290 Infinity II liquid chromatograph (Agilent, CA, USA) was equipped with a pentafluorophenyl (PFP) Poroshell 120 column and coupled to an Agilent 6470 triple quadrupole mass analyzer operating in positive ionization mode. Mobile phase solvents included H_2O with 0.1% formic acid (FA) (A) and acetonitrile with 0.1% FA (B). The analysis operated with a flow rate of 0.300 mL min^{-1}. Mobile phase conditions began at A-80%/B-20% and transitioned to A-5%/B-95% over 10 min. Analyte concentrations were determined from a nine-level calibration curve ranging from 0 to 200 μg L^{-1}. Blanks consisting of methanol (MeOH) with 0.1% FA were run between each calibration point and sample injection.

Stubs with carbon adhesive designated for LC-MS/MS analysis were extracted using a method previously reported in our group.[6,15–17] Six aliquots of 50 μL MeOH were deposited onto the stub. Each aliquot was deposited and withdrawn six times to ensure effective extraction of the stub. This extract was filtered through a 0.22 μm microcentrifuge filter then dried down under a steady stream of N_2. Due to the expected low concentrations of OGSR to be recovered from the bystander and passerby, these residues were reconstituted with 50 μL of MeOH with 0.1% FA and 150 μg per L D_{10}-DPA (internal standard) for analysis.

Individual samples taken from the hands of the shooter, bystander, and passerby were analyzed by LC-MS/MS and SEM-EDS. These samples consisted of a GSR stub holder and aluminum pin with 50% of the pin covered with a half-circle of carbon adhesive (for SEM-EDS analysis), while the LC-MS/MS half-circle was positioned on top of a layer of single-sided tape. This allowed for removal of the LC-MS/MS portion, which was then transferred to another surface for extraction to avoid possible interferences between the two analysis procedures or extraction methods. Split samples analyzed in this manner were collected for all residues recovered from hands of the POIs in outdoor and vehicular settings and for 18 of 36 indoor samples to provide a more direct comparison between SEM-EDS and LC-MS/MS results.

Passive deposition stubs with STRAT-M synthetic skin were extracted by removing the synthetic skin with a pair of tweezers. This was cut into 10 small sections and submerged in 500 μL of MeOH. The exhaustive extraction was finished by sonicating the mixture for five minutes. This extract was removed, dried under a steady stream of N_2, and reconstituted with 50 μL of MeOH with 0.1% FA and 150 μg per L D_{10}-DPA (internal standard) for analysis.

2.3.3.2. SEM-EDS instrumental analysis. SEM-EDS analysis was performed using two systems. Passive deposition and pre-concentrated stubs were analyzed using a JEOL 6490LV (JEOL, MA, USA) following ASTM E1588-20 for GSR analysis.[14] The instrumental parameters used for spectral collection and analysis were an accelerating voltage of 25 kV, a spot size of 60, a working distance of 11 mm, and a magnification of 500×. To collect elemental information, an Xplore 30 EDS (Oxford Instrument, England) detector was used. Samples collected from individuals' hands were analyzed using a JEOL IT-510 SEM equipped with an Oxford Instruments UltimMax 65 EDS detector. Instrumental parameters were set to an accelerating voltage of 25 kV, spot size of 60, a working distance of 10.2 mm, and a magnification of 500×. Samples were mapped using automated software to collect for "characteristic", "consistent with", and "commonly associated with" particles. To image GSR particles, backscatter and secondary electron detectors were used. Mapping of samples was completed sequentially on approximately the entire area for whole 12 mm carbon stubs. For samples where 50% of the carbon stub was removed for LC-MS/MS analysis, a 40% area termination setting was enabled to not go past the carbon edge and reduce potential charging. No sample coating was applied to SEM-EDS samples within this study.

2.3.4. Data analysis. Particle counter data was recorded with an in-house LabView code and exported as a Microsoft Excel file. APS data was recorded using Aerosol Instrument Manager software (TSI Incorporated, Shoreview, MN, USA). Particle counts and sizes were then exported as a text file to Microsoft Excel for further analysis. After processing, statistical analysis was performed using JMP Pro statistical software (version 17.0.0) and R studio (version 2023.03.0 + 386). LC-MS/MS data analysis was performed using MassHunter Quantitative Analysis 10.0 (Agilent). SEM-EDS data analysis was completed in Oxford Instrument Aztec software (version 6.1). High-speed video was processed using Photron Fastcam Viewer (Photron, Tokyo, Japan). Low-speed video was processed using Davinci Resolve (Blackmagic Design, CA, USA). Blender (version 4.1) was used for producing models of the instruments and sensors used in the study.

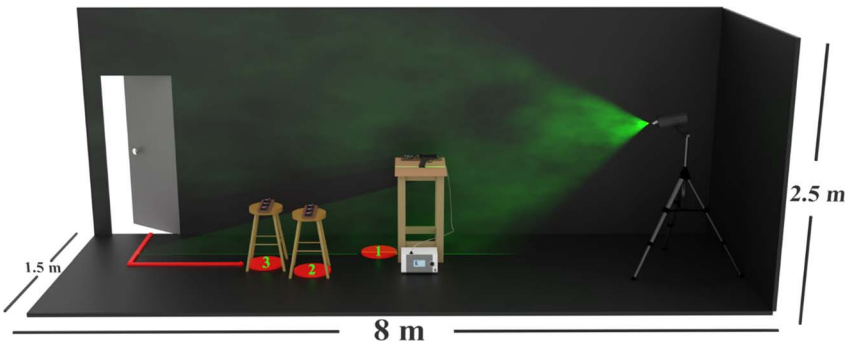

Fig. 3 Model depicting the positions of the shooter (1), bystander (2), and passerby (3). Additionally, the positions of the firearm, APS, particle counters, and laser sheet are shown. The individuals of interest were located next to the particle counters shown in the diagram. The bystander stood approximately one m behind and 30 cm to the right of the shooter, while the passerby stood directly behind the bystander.

2.4. Facilities and general experimental setup

2.4.1. Indoor experimental setup. All indoor shooting experiments were performed at West Virginia University's indoor Ballistic Testing Laboratory. A Springfield XD-9 9 mm pistol was used for the majority of the particle counting and analysis portion of this study. A Taurus model 905 9 mm revolver was used for ESI and comparison.† Factory-loaded Winchester Target and Practice 9 mm full metal jacket ammunition was used.

A 1.4-m-high shooting rest was constructed to provide a repeatable position from which the operator could fire. The positions of the particle counters, APS, laser sheet and operators are shown in Fig. 3.

The collection apparatus shown in Fig. 4 was constructed to allow a user to carry multiple types of collection equipment at once and to ensure the repeatability in placement of the collection equipment through multiple trials. SEM stubs with carbon adhesive tape were placed into holders in three locations on the apparatus. These stubs would remain in place following a shooting event, allowing for passive collection (deposition) of both IGSR and OGSR on the carbon adhesive. The stubs were analyzed by LC-MS/MS and SEM-EDS. Also, one stub (analyzed by LC-MS/MS) had a small section of STRAT-M synthetic skin adhered to the carbon tape to mimic deposition on skin. STRAT-M has been shown in previous studies from our group to have similar behavior to human skin for the purposes of OGSR and IGSR deposition.[32] In addition to the passively collecting stubs, two carbon adhesive stubs were held in 3D-printed molds 2 mm away from the outlet of the custom-made particle counters. These are designated as "preconcentrated" stubs and allow for capture of particles that exit from the particle counters. The purpose of the preconcentrated stubs was to ensure that the particles being counted, which were sampled at the exit of the counter, were in fact GSR and not other airborne particles. Since the device is collecting particles using a more dynamic process at the exit of the device flow (rather than a static setting), it was used to investigate a possible novel means of atmospheric GSR collection. Preconcentrated stubs were analyzed by SEM-EDS. Additional information and results concerning the preconcentrated stubs can be found in the ESI Section.† Additionally, residues from the hands of the persons of interest (shooter, passerby, and bystander) were collected using standard protocols with carbon adhesive stubs and analyzed by SEM-EDS and LC-MS/MS.

2.4.2. Outdoor and semi-enclosed experimental setup. All outdoor and vehicle experiments were conducted at the Monongalia County Shooting Range. Within these experiments, the same shooting rest, particle counter holders, and participant positions were replicated as closely as possible, as shown in Fig. 5. As outdoor shooting ranges are often less restricted in caliber and firearm ratings, a wider range of firearms was used. These included one pistol (Springfield XD-9, Winchester Target & Practice 9 mm), one revolver (Smith and Wesson 686-6, Winchester .357 Magnum), one shotgun (Winchester Defender,

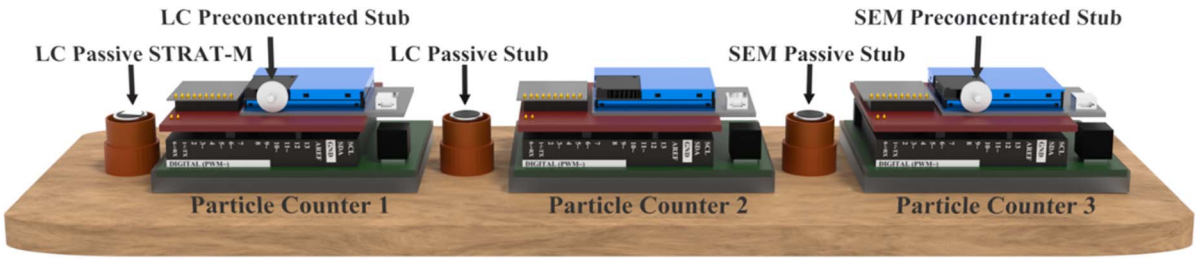

Fig. 4 Model showing the multi-method sampling device, used to carry three custom-made particle counters as well as passive collection carbon adhesive stubs and stubs affixed closely to the particle counter outlet, on which GSR that passed through the particle counters could be collected.

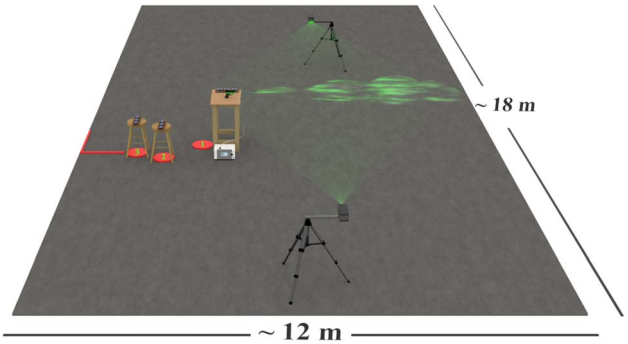

Fig. 5 Model showing the positions of the shooter (1), bystander (2), and passerby (3) at the outdoor range. In these experiments, two laser sheets were used and were positioned horizontally to illuminate a wide area. The positions of the particle counters and APS relative to the involved individuals remained the same as in the indoor portion of the study.

Remington Magnum Buckshot 12 ga.), two rifles (DPMS AR-15, Winchester M855 5.56 × 45 mm NATO and Kel-Tec RDB, Winchester M855 5.56 × 45 mm NATO), and one muzzleloader (Traditions Deerhunter .50 caliber, Pyrodex RS Powder). All ammunition within this study used standard leaded primers.

2.5. Experimental designs

2.5.1. GSR production and flow dynamics. A series of studies were conducted in an indoor shooting facility to determine vital characteristics of the GSR plume flow and distribution. Four particle counters were placed by the firearm discharge site for collection near the shooter. An additional sampler was placed at the rear of the room, four m behind the firearm, to determine the distance at which the GSR plume could spread. The APS was positioned next to the barrel of the firearm to count particles close to their point of generation. Both high-speed and low-speed videos were recorded in these studies in combination with the laser light sheet. A revolver and pistol were used in this study to investigate differences in the counts and distributions of particles produced by each firearm. The effects of airflow and ventilation were also investigated by enabling or disabling the range purification system to determine the possible sources of interference as well as evaluate the ability of the range to effectively purge itself of suspended GSR after finishing data collection for each trial. Select experiments were also conducted in a semi-enclosed and outdoor setting with additional firearms (Fig. 2A1–A3). Variables of interest included the type of firearm, the presence of airflow (range ventilation), and distance from the shooting point.

2.5.2. Duration of airborne GSR suspension. Extended samplings of the GSR plume were conducted to determine the settling rates of GSR particles following an indoor shooting event (Fig. 2B). In this experiment, the sampling apparatus shown in Fig. 6 was used. The APS input tubing was positioned directly beside of the shooting position (within 15 cm of the firearm barrel). The APS was programmed to record sections of data in one-min intervals for five h. The particle counters were activated and allowed to record for the same length of time. The

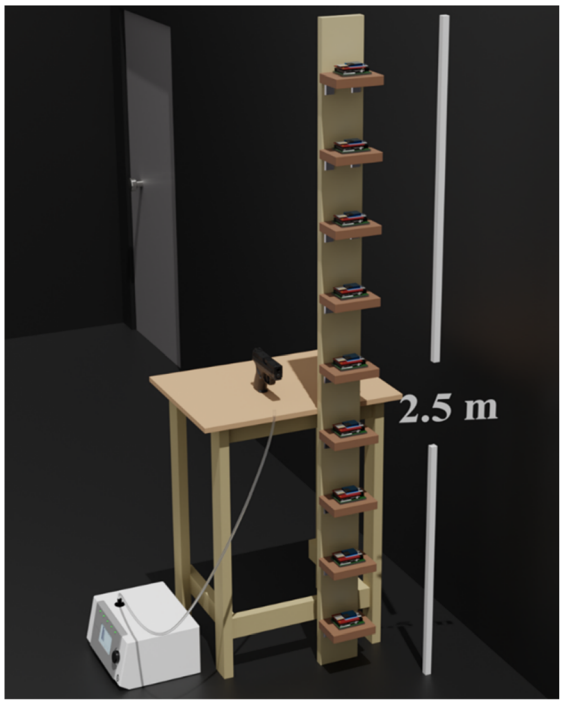

Fig. 6 Model of the sampling apparatus used to monitor the duration of airborne GSR suspension, in which a series of particle counters are fixed at different heights.

shooter fired one shot, began recording data, and immediately left the range while moving slowly to ensure that minimal airflow disturbance occurred. The door was closed and locked, and the range was left undisturbed for the five-h data collection period. Two trials were performed with particle counter data collection, and one of those trials also incorporated APS data collection. The ambient temperature was recorded at 2 °C for the duration of the experiments.

A similar setup was utilized for the outdoor experiments. In this case, the firearm, APS, and multi-sensor approach were kept in the same position. The shooter fired a single shot and then remained stationary until all sensors returned to baseline counts. Samples were collected in this manner using multiple calibers, including 9 mm, .357 magnum, 12 ga., 5.56 × 45 mm NATO, and .50 caliber black powder. A total of three trials were conducted with each firearm.

To simulate drive-by shootings, GSR flow and deposition were investigated in a semi-enclosed environment of a full-size truck (2018 Chevrolet Silverado, crew cab) and small sedan (2016 Volkswagen Jetta), with all windows closed except for the front passenger. The shooter was positioned in the driver's seat and aimed the firearm out the front passenger window.

2.5.3. IGSR and OGSR deposition on a shooter, bystander, and passerby. Passive collection stubs were placed by the respective particle counters for each location and analyzed by SEM-EDS ($n = 12$) and LC-MS/MS ($n = 15$). In addition to the passive collection stubs, samples were collected from the hands of the shooter, bystander, and passerby. Hand samples were taken by stubbing the individual's thumb, index finger, and

thenar region of the palm 20 times on the front and back of both hands. Hand samples were analyzed by LC-MS/MS ($n = 36$) and SEM-EDS ($n = 18$). The APS was placed in three locations (shooter, bystander, and passerby) throughout the study for a total of $n = 15$ samples. Finally, laser sheet scattering coupled with low-speed videography was performed. In this instance, the laser light sheet was rotated 90° to form a horizontal plane. The shooter was positioned in a chair so that the barrel of the firearm coincided with the light sheet. In the low-speed video (only), the bystander was instead positioned to the left of the shooter due to constraints in the design of the laser's tripod. The shooter and bystander were positioned one meter apart from one another.

To expand the information gained from this study, airborne particle sampling was performed (APS $n = 9$, particle counters $n = 81$) and samples were taken from the hands of a shooter, bystander, and passerby (LC-MS/MS $n = 27$, SEM-EDS $n = 27$) in an outdoor environment using the same firearm and ammunition. In the outdoor experiments, the particle counters and APS were kept in the previously described positions, as shown in Fig. 5. The shooter, bystander, and passerby followed the same protocol, with the exception that the passerby was not separated from the shooting event by a wall. Instead, the passerby remained at a distance of >15 m behind the shooter before moving into position following each shot.

Finally, the deposition of GSR on a shooter and bystander was repeated in two vehicles. In these studies, the APS ($n = 8$) was positioned at the lower edge of the passenger window. At the same time, the particle counters ($n = 80$) were placed in various locations, including the driver's dashboard, the passenger's dashboard, the inside passenger door, the center consoles, the rear passenger seat, the rear center seat, the rear driver's headrest, the rear center seat, and the rear driver's seat. In this scenario, hand samples were taken from a shooter positioned in the driver's seat ($n = 5$) and two bystanders positioned in the rear driver's and passenger's seat ($n = 5$ per passenger), while the car remained stationary due to safety concerns.

3 Results and discussion

3.1. GSR production and flow dynamics

The purpose of this experiment was to answer key questions about the nature of GSR and its interactions with atmospheric sampling systems. In particular, the size and distribution of particles released by different firearms and under various environmental conditions were evaluated.

3.1.1. Effect of environmental conditions on GSR particle sizes and distributions. First, GSR particle sizes and distributions were evaluated before, during, and after the discharge of the firearm indoors. With the APS and particle counters in the positions detailed in Fig. 2, the particle counts, sizes, and distributions were recorded after firing one shot with a Springfield XD9. The resulting APS size distributions can be observed in Fig. 7. From the APS results, a distribution of particles with the mean centered at approximately 1.8 μm range is observed. This is consistent with current methods for analysis of IGSR by SEM-EDS, which are often set up with a lower particle size limit

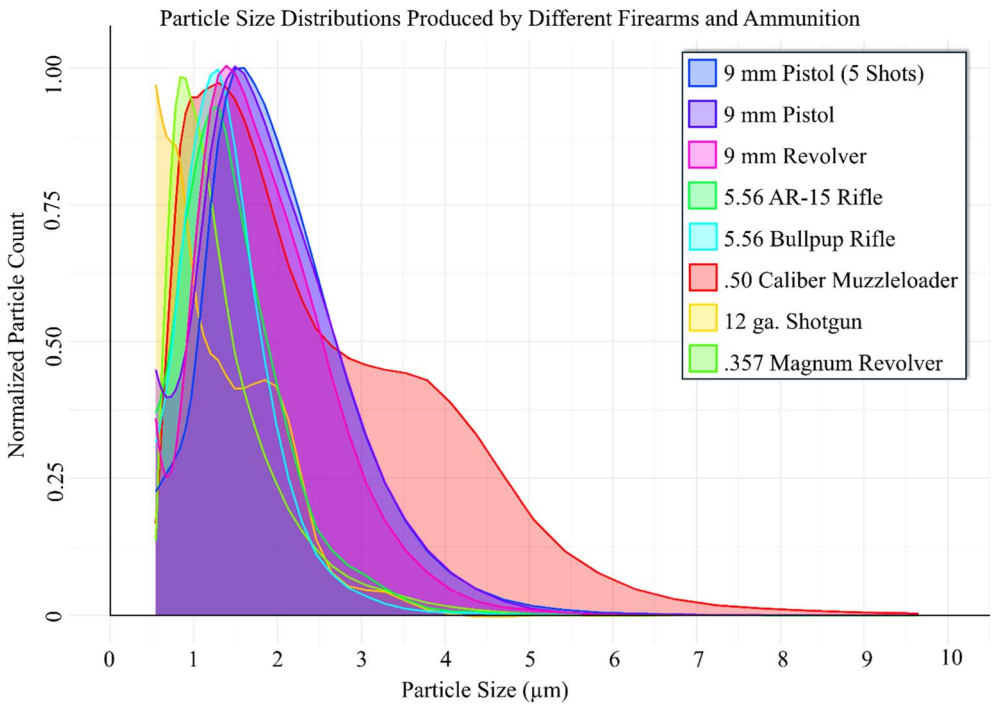

Fig. 7 Comparison of size distributions of particles counted by the APS using different firearms and ammunition. Particle counts were normalized to account for differences in magnitude caused by (1) shot-to-shot variability and (2) differences between firearms to highlight similarities and differences in size distributions. Counts from particles <0.523 μm have been removed from the plot due to the bin size being significantly larger than other bins, resulting in skewing of data.

of one μm. The distribution also shows that most particle sizes range from 0.5 μm to 1.8 μm.

Next, the similarities and differences in particle distributions between a revolver and pistol firing the same ammunition were evaluated. This information can be critical in formulating and evaluating hypotheses of how a criminal event evolved, depending on the type of firearm. Fig. 7 demonstrates that both a revolver and pistol produce particles of a similar size distribution range. Therefore, it was determined that neither the length of the barrel (5.1 cm revolver *vs.* 10.2 cm pistol) nor the type of firearm action have significant impacts on the sizes and distribution of particles observed under controlled collection sites, ammunition, and environmental conditions. Due to this finding, the pistol was used for the remainder of the indoor experiments. High-speed video was recorded for both the pistol and the revolver and can be seen in Video S1 of the ESI.† It is important to note that during these experiments, the particle collection sites were fixed at 15 cm to the left of the muzzle of the firearm. As semi-automatic pistols typically eject empty cartridges to the right, it is possible that the overall count and distribution of particles could show slight differences if the sensors were positioned at this location. The revolver's cylinder gap could also play a role in dispersing GSR in a sideways manner as well.[36]

The effect of the number of shots fired was evaluated given that this information could also play an important role in evidence interpretation. Using the pistol, five replicate experiments were performed by firing both one and five shots. No major difference was observed in the distribution of particles, but the number of particles was determined to be greater when firing five shots. High definition, low-speed video was recorded for both types of trial and can be seen in Video S2 of the ESI.†

The outdoor shooting range allowed for a larger variety of firearms to be tested in addition to pistol and revolver. As can be observed in Fig. 7, the particle size distributions for both 5.56 × 45 mm rifles were comparable to one another, despite the differences in action design. In the AR-15 style rifle, the action is located near the shooter's hand and is considered an "open" design. In contrast, the action on the bullpup-style rifle is positioned near the shooter's shoulder below the stock of the firearm and is considered a more "closed" design. However, these differences in characteristics had no easily observable effects, supporting and furthering the conclusion that the size distribution of suspended particles following a firing event is more likely to be dependent on the caliber of ammunition, rather than the action type.

The .357 Magnum revolver, 12 ga. shotgun, and .50 caliber muzzleloader all produced particle size distributions with noticeably different characteristics in comparison to the other firearms used in this study. The .357 Magnum revolver produced a similarly shaped distribution, but with the maximum centered below one μm. The 12 ga. shotgun produced a distribution in which the maximum was determined to be less than 0.523 μm, which is very different from the other firearms used in this study. Finally, the .50 caliber muzzleloader produced larger particles that were observed above baseline with a size greater than six μm. However, it is important to clarify that, unlike the other firearms used, the muzzleloader's propellant is Pyrodex, having an entirely different chemical makeup than smokeless powder and should be expected to produce different results. Videography of the GSR plume of all outdoor-only firearms discussed in this section can be viewed in ESI Videos S3–S10.†

3.1.2. Effects of ventilation on the GSR plume and airborne GSR dissipation. The particle counters and videography (Fig. 8) were used to evaluate the ability of the indoor range ventilation system to adequately remove GSR from the air. This was important to ensure that each sample started with a clean atmosphere and to establish the baselines when low background levels of particles were monitored. Turning on the ventilation system between experiments also guaranteed that the particulate observed after firing was coming from GSR residues produced during each firing event rather than other airborne particulate. Within approximately 20 s of the air purification system starting, particle counts returned to baseline levels (Fig. 9). The difference in GSR plume persistence can be readily observed using laser sheet scattering coupled to videography. Fig. 8 and Video S11 of the ESI† shows particulates rapidly exiting the range (upward) into the ventilation system when it is on. Therefore, the results demonstrated that the range was clean prior to the start of each sample when the ventilation system was run for at least one min between trials. For outdoor experiments, the signals of the APS and samplers were monitored to reach a baseline before every firing event.

3.1.3. Effect of indoor, outdoor, and vehicular spaces on GSR diffusion. The ability of GSR to spread within an enclosed room was evaluated to determine risks of exposure and potential deposition of residues onto surfaces or individuals in the room. Particle counters were placed 15 cm to the left of the muzzle of the firearm and at the back of the room at a distance of four m behind the shooter. Counters near the shooter began to show particles within seconds (<10 s) following each shot. After a period of 112 ± 34 s, the counters at the back of the room began to show particles, which were also visible through the laser sheet path. Interestingly, airborne particle counts between both locations were comparable (2389 ± 501 particles per cm^3 near the firearm, 2106 ± 428 particles per cm^3 at the back of the room). This finding was critical to this study, as further experiments were based on the premise that the GSR plume can quickly move throughout an enclosed space. GSR may deposit on surfaces far from the firing event if given enough time to spread and under relatively undisturbed conditions in an enclosed space.

Comparatively, the GSR plume in an outdoor environment diffused in a similar manner, but the movement and dissipation were much faster than in an indoor environment and dependent on the direction and speed of the wind. During the outdoor experiments, wind speeds were recorded at less than 1.6 km h^{-1}. In a similarity to the indoor experiment, the GSR plume began to spread to fill the open space. However, before the cloud was able to spread in an appreciable manner, it was rapidly carried away by any ambient wind. This can be observed in Fig. 10 and in Videos S12 and S13.†

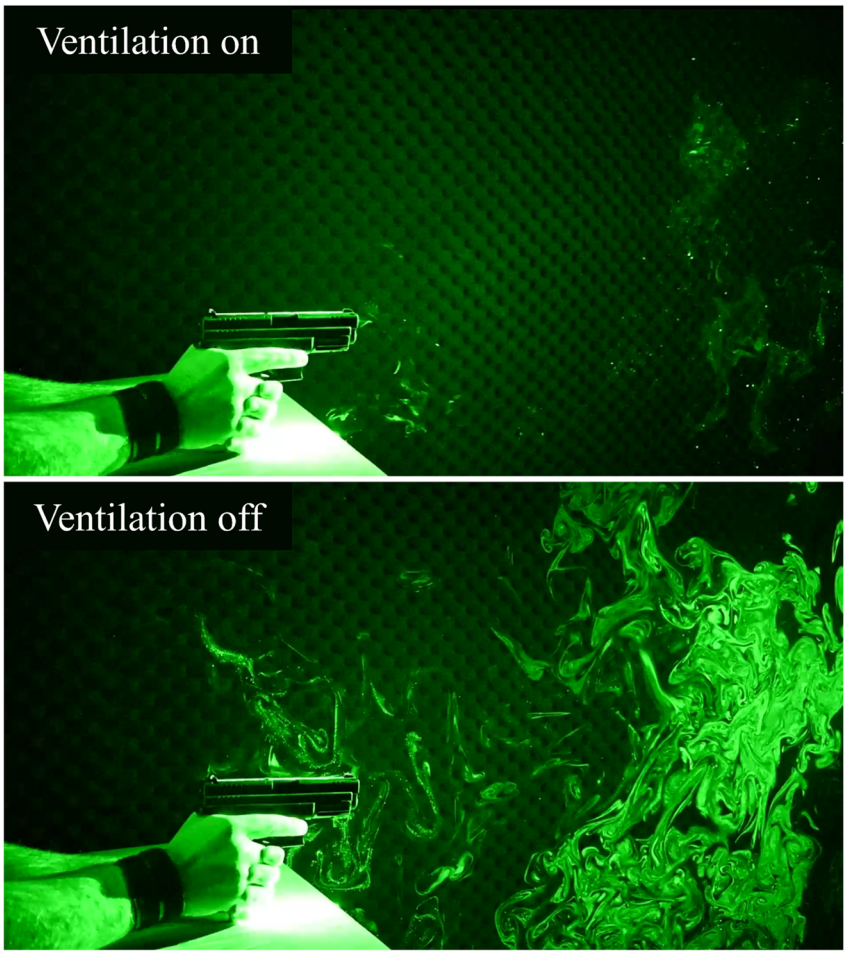

Fig. 8 Demonstration of the effects of ventilation on GSR flow. This image shows illuminated GSR particles observed in trials with the ventilation active (top) and the ventilation disabled (bottom). This image was captured five s following a single shot.

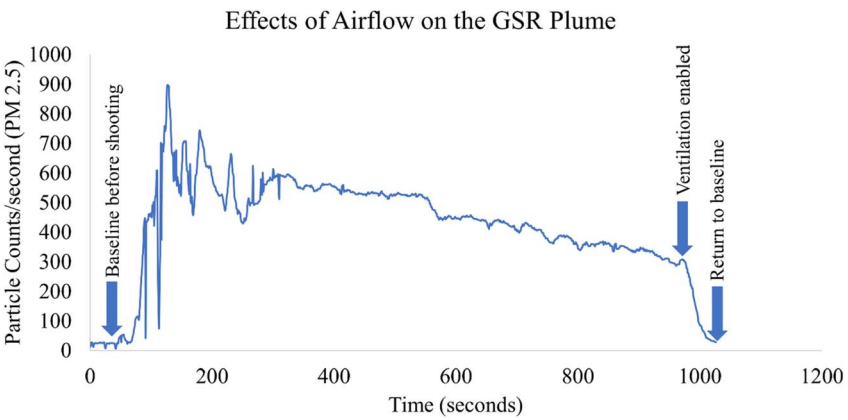

Fig. 9 Particle counter analysis of the effects of controlled airflow on GSR suspended in-air. Units include the number of particles less than 2.5 μm counted each second. When the ventilation is enabled, particle counts quickly return to their baseline value.

To investigate the characteristics of a drive-by shooting, the effects of airflow on GSR movement were studied in a vehicle. In this environment, videography (ESI Videos S14 and S15†) was performed during the semi-enclosed firing events from three perspectives, of which a still image can be seen in Fig. 11. The videography highlights important characteristics of GSR flow inside of a vehicle otherwise undetermined by other methods, in which the findings show that GSR inside of the vehicle behaves similarly to the indoor studies but with a rapid escape of GSR through the open passenger window. In this case, the

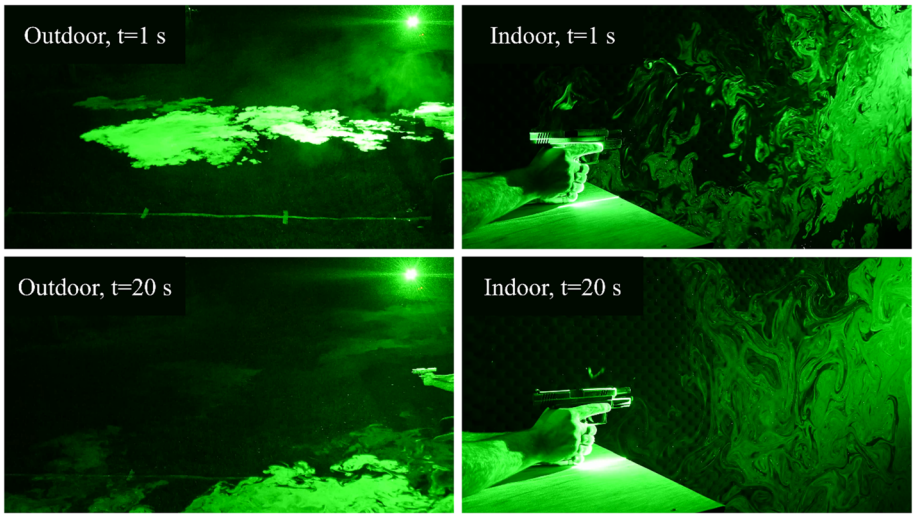

Fig. 10 Comparison of the diffusion characteristics of the GSR plume in outdoor (left) and indoor (right) environments. Note that the GSR cloud produced outdoors is rapidly (within seconds) carried away by light (<1.6 km h^{-1}) airflow during the diffusion process, while the GSR cloud produced indoors remains in place, slowly diffusing throughout the room.

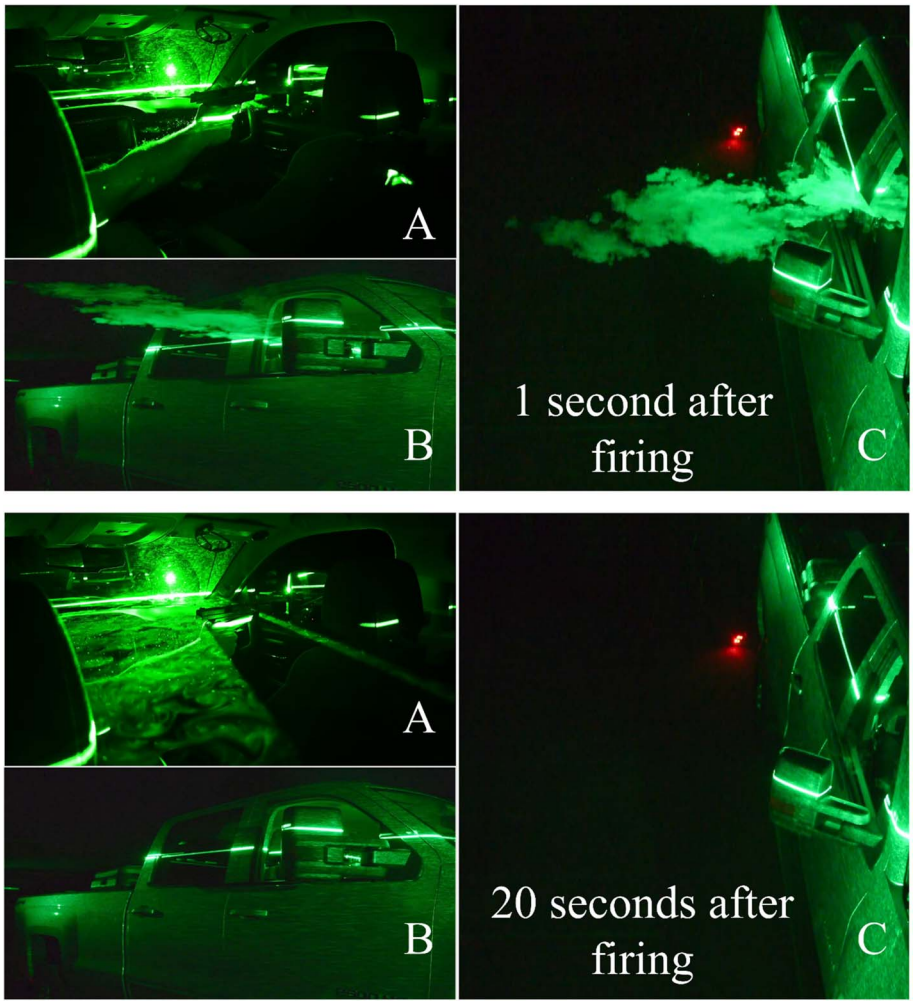

Fig. 11 Still images taken from three perspectives (A) inside of vehicle, (B) outside looking up, and (C) outside looking down at two different times: 1 s following firing (top) and 20 s following firing (bottom). Of note is the rapid permeation of GSR throughout the inside of the vehicle, which persists despite the outside GSR being quickly carried away.

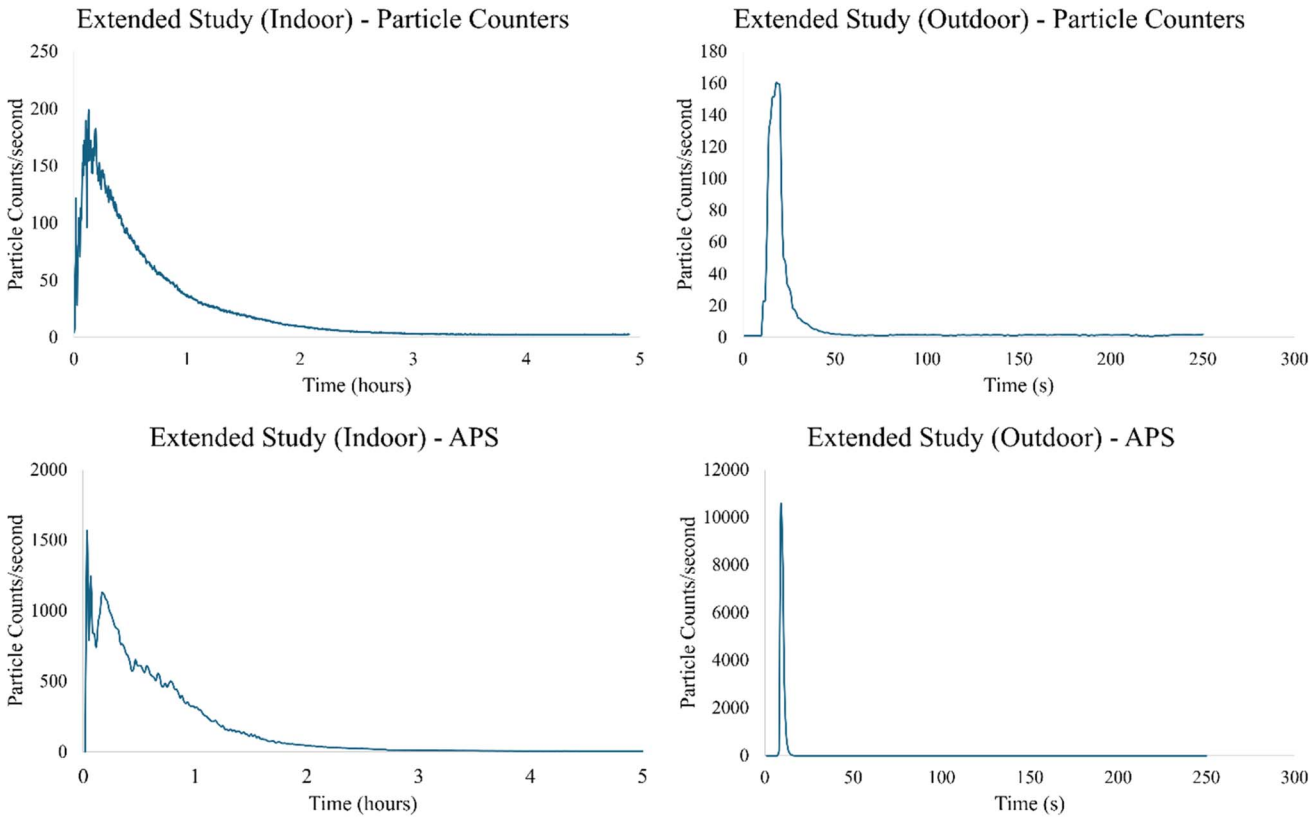

Fig. 12 Indoor formation and deposition patterns, measured by particle counters (top) and APS (bottom) over a five-hour sampling period in an enclosed range with minimal airflow (left) and an outdoor environment (right). During the indoor experiment, particle counts returned to baseline after approximately three hours. However, in the outdoor study, particle counts returned to baseline 45 s after firing (particle counters), and 10 s after firing (APS).

cloud slowly expands to fill the inside space. When the cloud meets the open window, it drifts outside, where its behavior shifts to match that observed in the outdoor studies. At this point, the GSR is carried away, as determined by the direction of the light (<1.6 km h^{-1}) ambient airflow.

3.2. Duration of airborne GSR suspension

The duration that GSR remained suspended in the air in different environments was another key question in this study. Suspended GSR has the potential to transfer to surfaces, including but not limited to additional persons passing through

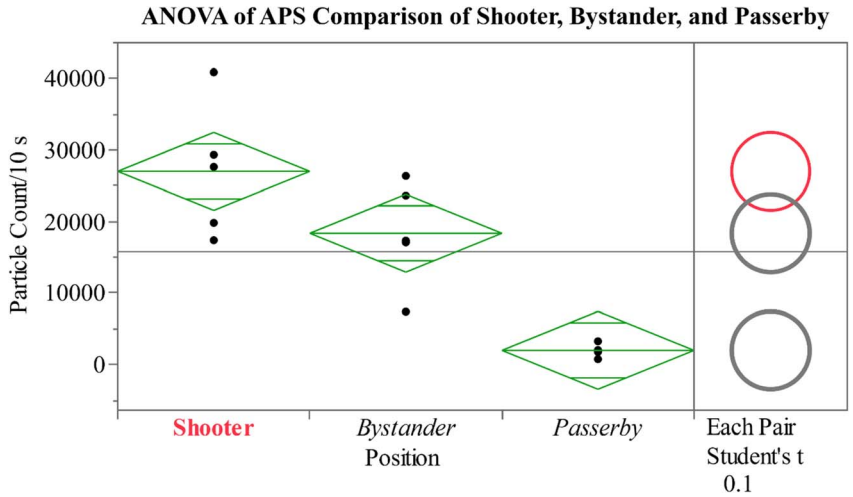

Fig. 13 ANOVA results from the comparison of overall particle counts observed by APS analysis. *T*-test results indicate that the shooter can be significantly distinguished from the bystander and passerby when considering $\alpha = 0.10$.

a crime scene long after the discharge of a firearm. The atmospheric counters revealed the extent to which IGSR and OGSR can move and then be deposited to substrates or persons in the indoor room and open spaces. Two atmospheric sampling methods were employed in this experiment to cross-corroborate the results. When indoors, the APS showed particulate concentrations in the room returning to baseline levels after three hours (~three particles per s observed at baseline). The experiment was repeated with various atmospheric particle counters, corroborating the findings (Fig. 12). It is important to note that the APS operates at a higher flow rate than the custom-made particle counters. Additionally, the APS is set to record data in 60-s intervals, whereas the particle counters record data in one-s intervals. The data is then compared as the relative decrease of particles rather than absolute counts measured by each instrument, since the purpose in this case is to observe the decay of GSR after firing and until it reaches baseline levels. The long settling time of several hours has important implications in the possibility of inadvertent transfer to a person long after the discharge of a firearm and without the person touching any surfaces on which GSR may be present. These experiments were performed at low ambient temperatures (2 °C) in an enclosed

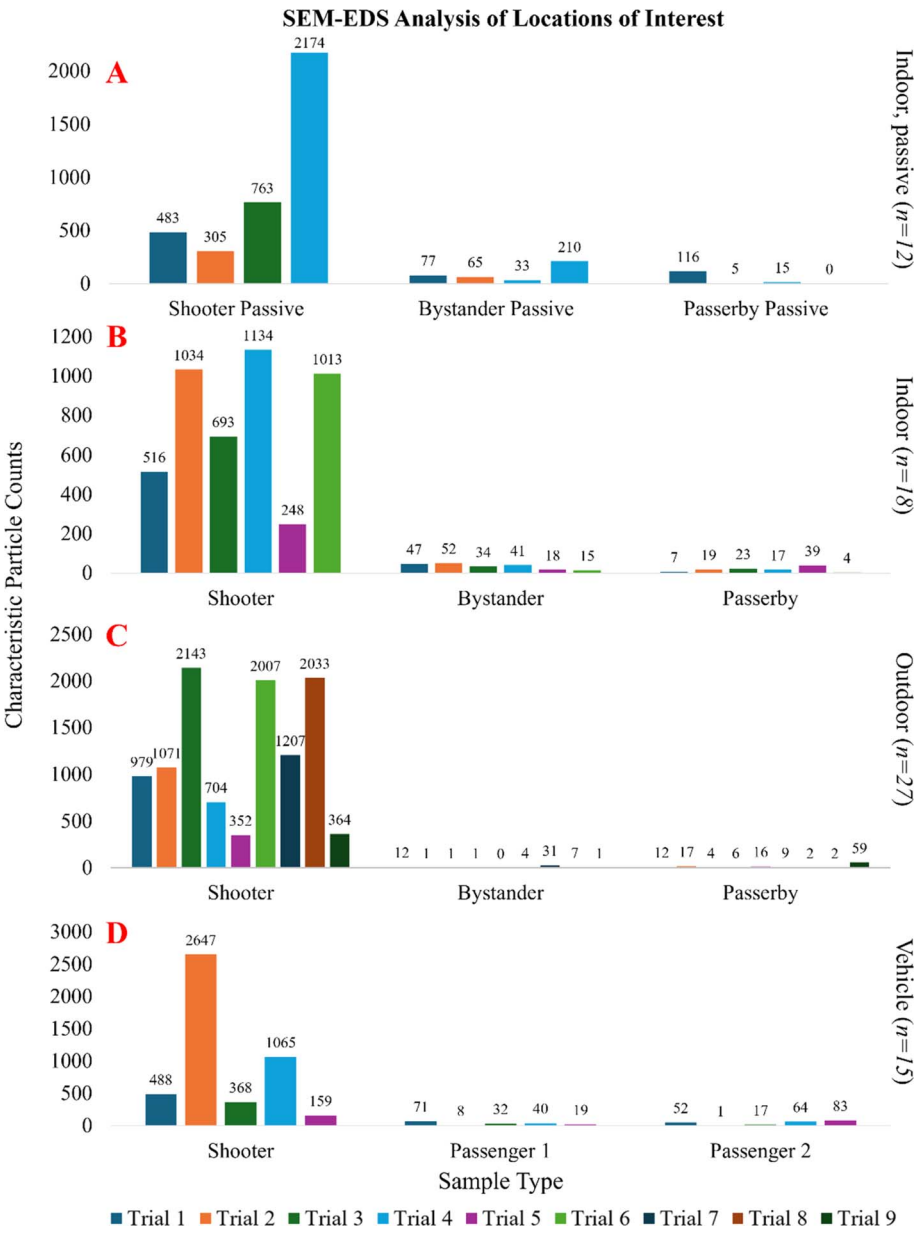

Fig. 14 Characteristic (containing Pb, Ba, Sb) particle counts analyzed by SEM-EDS. Passive samples were carbon adhesive stubs exposed to the GSR and intended to reflect passive deposition on a surface, which were placed in the locations of the shooter, bystander, and passerby in an indoor environment (A). Hand samples were recovered from the hands of a shooter, bystander, and passerby in indoor (B) and outdoor (C) environments. Samples were recovered from a shooter and two passengers in a semi-enclosed environment (D, vehicle). Italicized "*n*" denotes total sample count.

environment. Therefore, it is feasible that different environmental conditions (*i.e.*, higher temperatures, differing humidity, or altered airflow) may result in different GSR settling rates.

The outdoor shootings revealed a substantially different deposition and settling process. First, the settling time was much faster (in a matter of seconds, rather than hours) even under low wind conditions (<1.6 km h^{-1}). Second, the movement of the GSR plume was shown to be dependent on the wind directionality and pattern. Finally, since the space is not confined, the GSR distributed quickly throughout the open space. The cloud grew tridimensionally at least 10 m in about one min while moving away from the firearm due to light ambient airflow. The findings indicate that while the amount of GSR produced at the point of discharge is expected to remain the same, there is a reduced risk of GSR exposure for bystanders and passersby in open than enclosed spaces due to the more rapid movement of the GSR plume.

3.3. IGSR and OGSR deposition on a shooter, bystander, and passerby

The question of whether an individual who retains GSR is the same person who fired the gun has been historically difficult to answer. Therefore, the purpose of this experiment was to assist the development of a comprehensive approach for that answer. This experiment investigates the transference of GSR from the point of discharge to three positions: shooter, bystander, and passerby. These positions were determined to be of high interest, as the investigation of differences between them and defining characteristics of each location can lead to decisions about an individual's involvement (or lack of) in a crime.

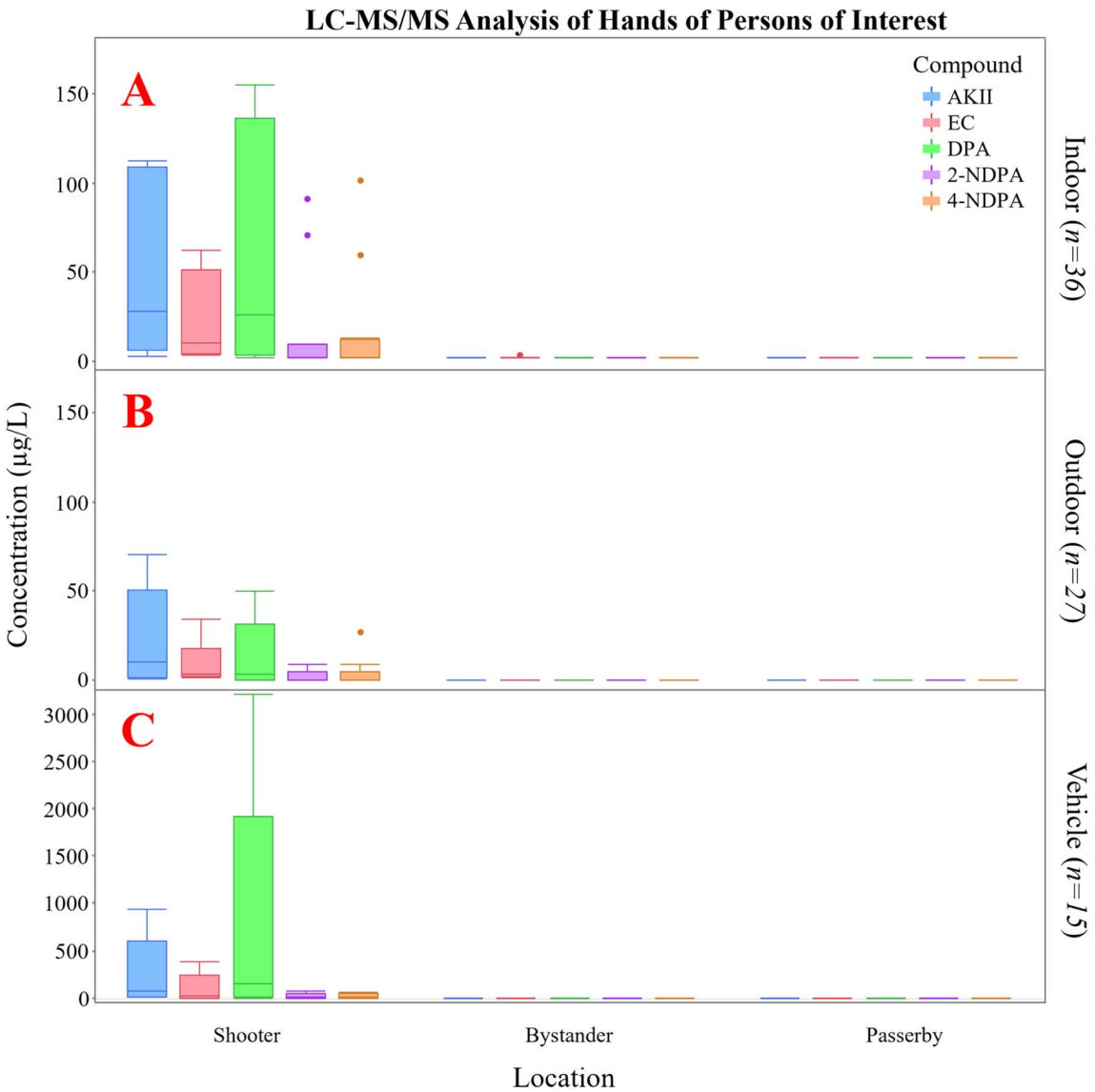

Fig. 15 Calculated concentrations of samples analyzed by LC-MS/MS. Samples were recovered from the hands of a shooter, bystander, and passerby in indoor (A) and outdoor (B) environments. Samples were recovered from a shooter and two passengers in a semi-enclosed environment (C, vehicle). Italicized "*n*" denotes total sample count.

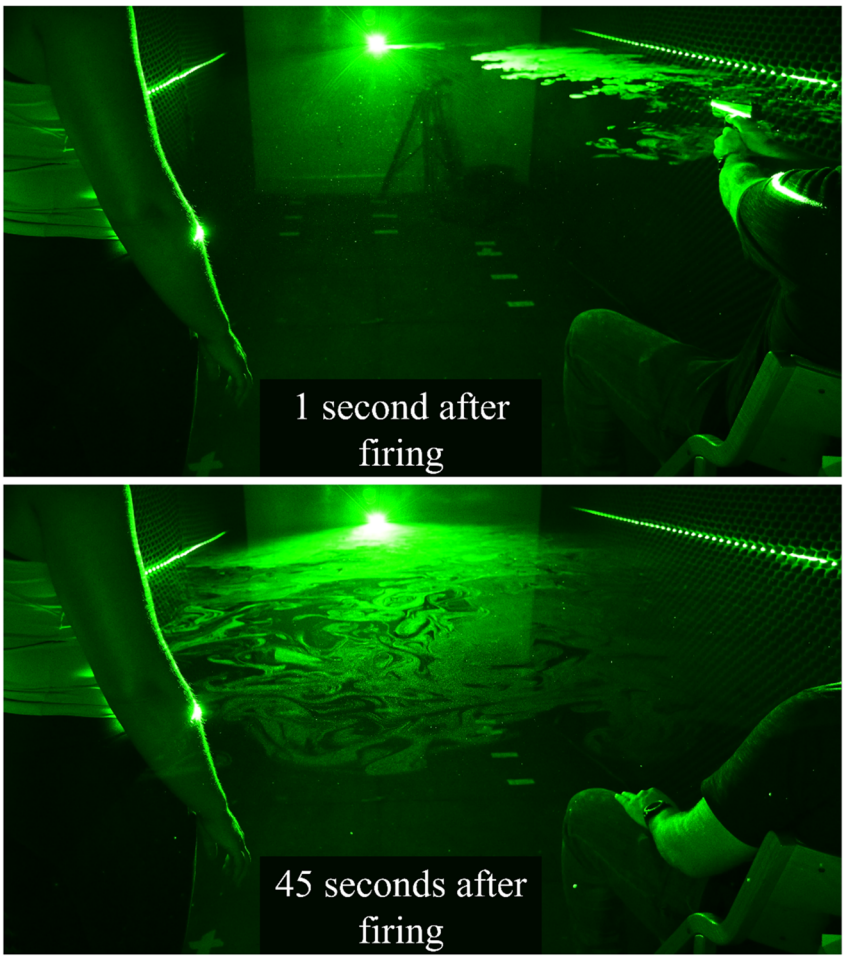

Fig. 16 GSR plume illuminated by horizontal laser sheet scattering immediately after firing (top) and 45 s after firing (bottom).

3.3.1. GSR deposition on a shooter, bystander, and passerby in an indoor environment. The purpose of this experiment was to determine the number of atmosphere-suspended GSR particles that an individual may be exposed to in three locations. In this experiment, the APS recorded particle counts every ten seconds for 15 minutes. Particle counts were recorded for the full 15-min duration of each trial regardless of the location of the APS. Total particle counts over the 90-sample trial were averaged to obtain average exposure amounts. Particle counts can be seen in Fig. 13. When considering a significance value (α) value of 0.10, significant differences in particle counts between each location can be seen with lower counts for bystanders and passersby as compared to shooters. This finding points to the idea that individuals in different areas relative to the firearm may receive varying degrees of GSR deposition. However, it is important to note that the firearm discharge in all locations produced particle counts above baseline level, except for some passerby trials. Therefore, it would be challenging to differentiate between each location if data for the remainder of the locations were not present or obtainable in a realistic scenario.

SEM-EDS was used as a confirmatory tool for the results presented in the APS analysis of the shooter, bystander, and passerby positions. While the APS was able to detect particles in all positions, it was still unknown whether these particles would remain suspended or deposit onto surrounding surfaces. Therefore, passive deposition stubs (carbon adhesive stubs left in place during and after firing, exposed to the GSR plume) were placed in each of the three positions ($n = 12$). The SEM-EDS results are presented in Fig. 14A. As depicted in the figure, passive deposition stubs located in the shooter position received more particles than other locations (within the same trial). However, in all but one trial, each stub received some level of IGSR deposition with both characteristic and consistent with GSR particles.

To further corroborate the risk exposure, samples ($n = 18$) were collected directly from the hands of the individuals in each location. Regardless of the location of the individual, each sample had at least one characteristic GSR particle detected, indicating that some exposure is possible to a bystander or passerby shortly following a shooting, even if the individuals had not made physical contact with any surfaces. These results are reflected in Fig. 14B. In similarity to the results obtained in APS analysis, SEM-EDS supports the findings in which we determined that the bystander and passerby locations are exposed to fewer particles than the shooter but are still likely to be exposed to some level of GSR.

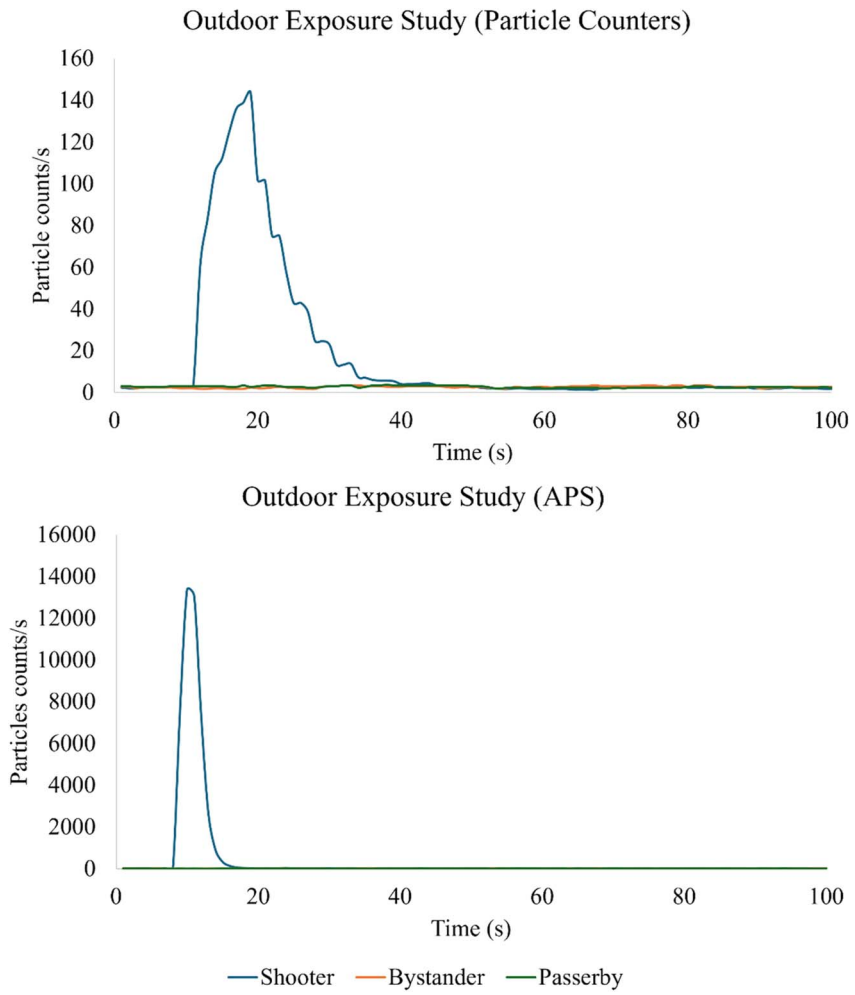

Fig. 17 Comparison of GSR exposure in three locations (shooter, bystander, and passerby) measured by particle counters (top) and APS (bottom) over a 100-second period. The particle counter responses consist of averaged values across three sensors located at each position.

While it has already been established that the bulk of particles detected by the APS and particle counting systems are inorganic, previous discussions and findings can still be evaluated for OGSR analysis. When passive deposition stubs were analyzed, no OGSR components were found above LOD (Table S1†) in any of the 15 samples collected on carbon adhesive. A similar trend was observed for those collected on synthetic skin. Low concentrations of AKII were detected on only one sample in the shooter's location. Given the fact that no appreciable OGSR was detected on samples even located directly beside the firearm, the conclusion can be made that the area of the stubs ($\sim$75 mm^2) may be too low for effective deposition and, therefore, deposited mass will remain under detection capabilities in most circumstances. Compared to traditional samples, *i.e.*, from the hands of the shooter in which the same type of stub is used for OGSR recovery, it is important to remember that the effective area for deposition is much larger.

As it has been determined that organic residues are not prone to passive deposition on carbon adhesive stubs, the hands of the shooter, bystander, and passerby were sampled across 12 trials ($n = 36$). These results are illustrated in Fig. 15A. In these trials, AKII, EC, and DPA were detected above LODs in all 12 of the shooter's hand samples. The increased rate of detection on hands *versus* passive deposition on nearby stubs with adhesive or synthetic skin is attributed to the larger superficial area sampled on hands (index and thumb areas) and the stronger contact of the adhesive with the skin during the collection process when compared to passive settling of organics on the surface.

In comparison, AKII, EC, and DPA were not detected in samples for the bystander and passerby's hands, except for one of the 12 samples that contained low levels of EC for a bystander. In contrast to the results from SEM-EDS analysis, it is evident that OGSR deposition from the firearm discharge to the hands of a bystander or passerby is unlikely. Moreover, the distinction between the shooter and non-shooters is clear when considering the OGSR. This suggests that the mechanism of deposition and transfer for residues of organic nature is highly dependent on the distance of the deposited surface and the surface area available for deposition.

The presence of OGSR compounds in high concentrations on a shooter's hand relative to concentrations on a bystander or

passerby's hand is a very significant finding. When comparing this finding to the results obtained for IGSR analysis, it becomes evident that the analysis of OGSR as a complementary tool provides new avenues for evidence interpretation. With the combined techniques for IGSR/OGSR monitoring, it is possible to enhance the confidence of results when attempting to determine if an individual of interest fired a gun or was merely present in the room during a firearm discharge.

To further understand these exposure and spread mechanisms, a video (ESI Video S16†) was taken with the laser sheet rotated 90° to form a horizontal plane that bisected the firearm barrel as well as the bystander's arm. The laser scattering uncovers the movement of GSR. After approximately 45 s, the GSR plume travels to the bystander and contacts the individual's arm. This contact persists for the remainder of the experiment. The visualization of GSR is shown in Fig. 16. This provides a final piece of evidence that GSR can travel from the firearm to a bystander, whether by the initial deflagration plume or by extended exposure to the slower-moving dense particle cloud when in an enclosed room with limited airflow.

3.3.2. GSR deposition on a shooter, bystander, and passerby in an outdoor environment. To provide complementary information to the indoor exposure studies, a set of samples (APS $n = 9$, particle counters $n = 81$, LC-MS/MS $n = 27$, SEM-EDS $n = 27$) were collected outdoors. In contrast to the studies performed indoors, the reduced GSR exposure in an outdoor environment is clearly observable by each method. This finding is supported by the differences in the flow patterns previously discussed.

Beginning with the atmospheric sampling methods, an example of the particle counts observed between the shooter, bystander, and passerby shortly following a firing event can be seen in Fig. 17. In the outdoor studies, no particle counts above baseline levels were observed for the bystander or passerby in any of the trials. Particle counts for the shooter's position were above baseline in all trials regardless of the air sampling method. In contrast to the indoor studies, in which the APS and particle counters would readily observe particles as GSR diffused throughout the room, the outdoor studies showed a clear distinction between the shooter's position and the

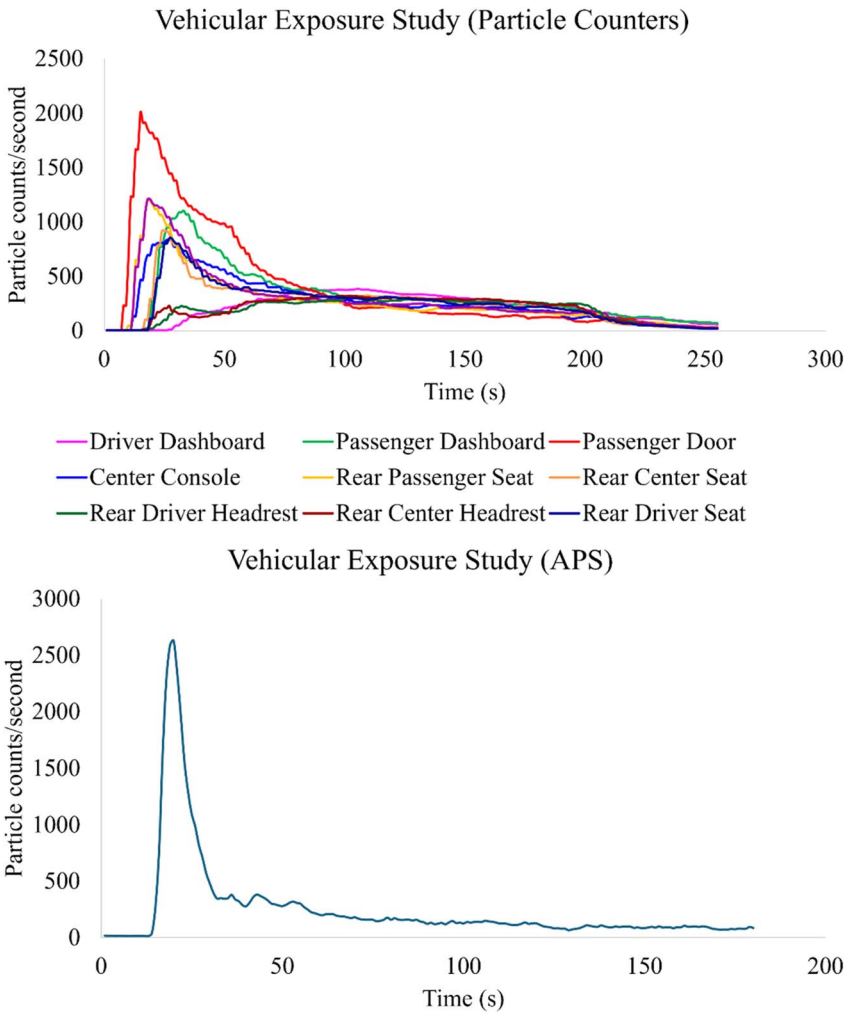

Fig. 18 Comparison of GSR exposure in a vehicle measured by particle counters (top) and APS (bottom). Particle counters were placed in various locations throughout the vehicle, while the APS was positioned with the inlet on the inside of the passenger window frame.

bystander/passerby. This is due to the behavior of the GSR plume in a truly open environment, even with <1.6 km h^{-1} of wind, where GSR is carried away and removed from the immediate location before it has had enough time to diffuse and reach the bystander or passerby at a level that is detectable by the atmospheric sampling methods used.

Samples taken from the hands of the shooter, bystander, and passerby were analyzed by SEM-EDS and LC-MS/MS. Results from SEM-EDS analysis can be seen in Fig. 14C. These results closely mirrored the indoor study, in which the shooter was likely to receive a high number of characteristic particles, while the bystander and passerby would receive fewer. The difference between counts of IGSR recovered from the shooter *versus* bystander and passerby was more abrupt outdoors, but again, it is important to note that in most trials, the bystander and passerby received some level of GSR.

LC-MS/MS results can be viewed in Fig. 15B. Similar to the indoor study, AKII and EC were detected on every hand sample from the shooter. However, no OGSR components were detected on either the bystander or passerby. These results follow the same trend observed in indoor settings, where the bystander and passerby are unlikely to receive OGSR deposition. This finding further confirms the hypothesis that combined OGSR and IGSR analysis can be utilized to determine if an individual of interest was the shooter, bystander, or simply a passerby during the commission of a crime.

3.3.3. GSR deposition on a shooter, bystander, and passerby in a vehicular environment. To evaluate a final environment that would closely replicate another drive-by shootings, the analysis of a shooter (driver) and bystander (passenger) was repeated in two vehicles. The results of the atmospheric sampling highlight interesting flow characteristics of GSR, an example of which can be seen in Fig. 18. Particle counters located closest to the firearm (*i.e.*, the passenger door) detected the greatest concentration of GSR, while those located further away (rear center headrest, driver dashboard, rear driver headrest) showed a delay in detecting particles. The behavior of airborne GSR inside of the vehicle can be closely related to that of the indoor studies, in which GSR quickly permeates throughout the enclosed area rather than being immediately carried away by ambient airflow, as was observed in the outdoor studies. This is supported by the finding that all particle counters, regardless of location, received some level of GSR exposure above baseline levels.

Samples taken from the hands of the shooter (driver) and bystander (passenger) analyzed for IGSR by SEM-EDS showed a trend that was similar to the indoor studies and can be seen in Fig. 14D. Across three trials, the passenger received some level of GSR exposure, although the shooter's hands received a greater number of IGSR particles than the bystander in each trial. This final piece of IGSR information again supports the conclusion that IGSR analysis alone may not be sufficient to distinguish between an individual who has fired a gun and an individual who was present during the firearm discharge, even if the passenger did not have physical contact with the shooter, firearm, or any other surface on which GSR was present.

The results indicate once more that OGSR was likely to be found in high concentrations on the shooter's hand yet unlikely to deposit on a passenger *via* airborne exposure (Fig. 15C).

4 Conclusions and future work

This study reports novel visualization and atmospheric sampling techniques for airborne GSR analysis combined with analytical techniques for chemical characterization of the recovered residues. Preliminary studies showed several key findings to understanding the production, deposition, transfer, and interpretation of IGSR and OGSR.

The novel technique of laser sheet scattering applied to GSR produced visually striking and highly informative results. In this study, particles far too small to see with the unaided eye were successfully revealed by the laser light sheet for visualization, and their spread and duration were monitored in real-time and space. GSR particle sizes observed through real-time atmospheric analysis were primarily between 1.4 μm and 1.8 μm, regardless of the number of shots and the type of firearm or ammunition, which confirms the capabilities of SEM-EDS for analysis of these residues. An exception to these generalized particle size distributions was observed for the 12 ga. shotgun (most particles were less than 0.523 μm) and the .50 caliber muzzleloader (produced particles > 6 μm).

The type of firearm did not have a substantial effect on the generation or movement of the GSR plume, although the distance from the shooter's hands plays a factor in the number and mass of recovered residues. Neither the length of the barrel nor the type of firearm action (*i.e.*, revolver *vs.* pistol) showed significant impacts on the particle sizes produced or the distribution of particles observed. GSR residues increase with the number of shots fired, but this increase is not necessarily proportional to the number of shots fired.

High airflow in indoor environments and outdoor wind were found to significantly affect the GSR plume spread, with the high-efficiency air purification system effectively removing airborne particles within approximately 20 s and even a mild outdoor wind dissipating the primary plume in less than one minute. The GSR plume was found to diffuse rapidly to fill available space, reaching locations as far as 4 m away in indoor environments in ~2 min, and >15 m away in approximately one min in the outdoors. In a semi-enclosed, vehicular environment, the GSR behaved in a manner that reflected a combination of indoor and outdoor observations. GSR within the vehicle was found to diffuse rapidly to fill the space while also escaping through the open passenger window. These findings provide critical information to evaluate the likelihood of finding GSR on persons or objects of interest, depending on the environmental conditions at the scene.

To this end, how long GRS is suspended in these environments is also relevant for interpreting the evidence. The setting time differences between indoor and outdoor conditions were substantial. For example, the duration of airborne GSR suspension was approximately three hours in undisturbed indoors under our experimental conditions. In contrast, in outdoor conditions the GSR remained in the air less than one

minutes, even with low (<1.6 km h^{-1}) wind conditions. This finding has considerable implications for the risk of contamination of a bystander or passerby long after a firing event. Of particular importance is to evaluate alternative methods of transfer to an individual not involved in a crime (*i.e.*, passerby) or involved but under different circumstances (*i.e.*, bystander *vs.* shooter). The risks of exposure to airborne GSR were more likely indoors than outdoors and much more likely for IGSR than OGSR, as corroborated by imaging, particle distributions, and chemical analysis.

The APS showed significant differences in particle counts for the shooter, passerby, and bystanders. Moreover, the particle counters were set up on devices that allowed simultaneous passive collection of GSR. The evaluation of passive deposition stubs for IGSR by SEM-EDS showed that GSR exposure of an individual either witnessing a crime or entering the area shortly after is probable. While the overall particle counts were lower than that of a shooter, it is important to note that a relative assessment of shooter *versus* non-shooter individuals may be difficult to obtain in a real-case scenario. To complement these findings, samples were taken from the hands of individuals involved in the firing event, producing similar results. In this case, the shooter received, on average, more particles than the bystander and passerby. However, in all but one sample, the bystander and passerby had at least one characteristic IGSR particle recovered from their hands despite not coming into contact with any surface.

On the other hand, OGSR deposition on passive collection stubs was found to be unlikely, again supporting the hypothesis that OGSR deposition decreases quickly with increasing distance from the firearm. The analysis of hand samples from a shooter, bystander, and passerby's hands by LC-MS/MS produced another significant finding. All shooter's hand samples were positive for at least three OGSR compounds, while the corresponding paired bystander and passerby samples were mostly negative, with only one compound (EC) being found in low concentrations on one of 12 bystander hand samples. This finding adds immense value to OGSR analysis as a practice, as it shows that OGSR transfers from the firearm to the shooter (even in outdoor settings), but it is very unlikely that OGSR transfers to an individual in the proximity of the shooter. Therefore, OGSR analysis, when considered in combination with IGSR monitoring, has the potential to assist with evaluating alternative hypotheses, such as the person of interest (POI) fired the gun *versus* the POI who was in contact with the crime scene but did not fire the gun (passerby, bystander, passenger, *etc.*).

Testing in an outdoor environment further evaluated the potential interferences that may arise in more realistic scenarios with less controlled variables (*i.e.*, natural airflow and environmental conditions at the time of the firing). The comprehensive study unveils, corroborated by multiple sensors, that GSR exposure risk for a passerby or bystander is lower in outdoor environments; thus, it is a crucial consideration that could be incorporated in evidence interpretation.

Drive-by shootings are another scenario that is commonly found in criminal investigations. The simulation in this study shows the imminent exposure of GSR for passengers in the vehicle and discovers the rapid spread of residues inside the vehicle and immediately outside open windows. The GSR plume dissipates much faster when exposed to the environment outside of the vehicle. It also shows that the differentiation of shooters *vs.* non-shooters in a car cannot be solely determined by GSR evidence recovered from the hands of the passengers.

Overall, this study documents the mechanisms of IGSR and OGSR production, transport, and levels of exposure using a multi-sensor approach that offers a one-of-a-kind unveiling and cross-corroboration of the factors affecting the dynamics of gunshot residues. First, the environmental and shooting conditions influence GSR production and flow dynamics. GSR rapidly expands from the discharge point to fill the open space. In indoor shooting, the GSR can move up to 4 meters away from the shooter in a few minutes and can remain in airborne for up to 3 hours under undisturbed conditions. In outdoor shootings, the GSR rapidly moves from the shooter to over 15 meters away in less than one minute. However, unlike indoors, the duration airborne GSR near the location of discharge lasts just a few seconds in outdoor settings, even with no perceptible windy conditions. These findings imply that the risk of exposure to non-shooters nearby or those who enter the scene minutes after is remarkably different if the firing happened indoors or outdoors. Notably, IGSR and OGSR are effectively deposited on the hands of the shooter, regardless of indoor, outdoor, or semi-enclosed conditions. However, only IGSR is likely to transfer in detectable amounts to the hands of passersby or bystanders, who have not touched or handled a firearm. Altogether, this study offers opportunities for the practitioner (scientists and lawyers) to utilize information about environmental and shooting conditions to evaluate the evidence under activity-level propositions. This can be more efficiently used if the laboratory incorporates protocols to assess the complementary information of IGSR and OGSR data. The study findings open new avenues to interpret GSR data applicable in forensic science and other disciplines where GSR can be an environmental or health concern.

Disclaimer

Certain commercial products are identified in order to adequately specify the procedure; this does not imply endorsement or recommendation by NIST, nor does it imply that such products are necessarily the best available for the purpose.

Data availability

Some of the video content from this work is available in the ESI section† and additional data will be made available upon request once the data archiving is approved by the funding agency for open access.

Author contributions

Thomas Ledergerber: conceptualization, methodology, validation, formal analysis, investigation, data curation, writing –

original draft, visualization. Matthew Staymates: conceptualization, methodology, software, investigation, resources, writing – review and editing, visualization. Kourtney A. Dalzell: methodology, validation, formal analysis, investigation, writing – review and editing, visualization. Luis E. Arroyo: conceptualization, methodology, investigation, resources, writing – review and editing, funding acquisition. Roger Jefferys: investigation, writing – review and editing. Tatiana Trejos: conceptualization, methodology, validation, investigation, resources, writing – review and editing, supervision, project administration, funding acquisition.

Conflicts of interest

The authors declare that they have no known competing financial interests or personal relationships that could have appeared to influence the work reported in this paper.

Acknowledgements

The authors would like to thank Dr Keith Morris for his assistance in collecting samples at the WVU's Department of Forensic and Investigative Science Ballistics Testing Facility. Additionally, the authors would like to thank the Monongalia County Sherriff's Office for allowing the use of the Monongalia County Shooting Range. Finally, the authors would like to thank Leah Thomas, Liliana Barbosa, Sharon Kalb, and Isabel Talley for their assistance in sample collection and processing. This project is sponsored by Award No. 15PNIJ-23-GG-04218-SLFO from the National Institute of Justice to West Virginia University. Instrumentation used in this project was also supported by award "60NANB22D204, Procurement of Technology and Equipment to Respond to Opioid and Violence Epidemics in WV" from the Department of Commerce to West Virginia University. The opinions, findings, and conclusions are those of the authors and do not necessarily reflect those of the Department of Justice or the Department of Commerce.

References

1 L. S. Blakey, G. P. Sharples, K. Chana and J. W. Birkett, *J. Forensic Sci.*, 2018, **63**, 9–19.
2 W. Feeney, C. Vander Pyl, S. Bell and T. Trejos, *Forensic Chem.*, 2020, **19**, 100250.
3 L. Garofano, M. Capra, F. Ferrari, G. P. Bizzaro, D. Di, M. Dell'olio and A. Ghitti, *Forensic Sci. Int.*, 1999, **103**, 1–21.
4 S. C. Smith, O. B. Black and C. Roper, *Appl. Sci.*, 2022, **12**, 1–18.
5 O. Black, S. C. Smith and C. Roper, *Ecotoxicol. Environ. Saf.*, 2021, **208**, 111689.
6 W. Feeney, K. Menking-Hoggatt, L. Arroyo, J. Curran, S. Bell and T. Trejos, *Forensic Chem.*, 2021, **27**, 100389.
7 J. E. Wessel, G. M. Wolten, P. F. Jones, M. H. Mach, R. S. Nesbitt, A. R. Calloway, A. Pallos and L. Operations, *Equipment Systems Improvement Program: Symposium Synopsis Detection of Gunshot Residue*, 1975.
8 G. M. Wolten, R. S. Nesbitt, A. R. Calloway, G. L. Loper and P. F. Jones, *Aerospace Report No. ATR-77(7915)-3 Equipment Systems Improvement Program: Final Report on Particle Analysis for Gunshot Residue Detection*, 1977.
9 E. Goudsmits, G. P. Sharples and J. W. Birkett, *Sci. Justice*, 2016, **56**, 421–425.
10 A.-L. Gassner, C. Ribeiro, J. Kobylinska, A. Zeichner and C. Weyermann, *Forensic Sci. Int.*, 2016, **266**, 369–378.
11 C. Hofstetter, M. Maitre, A. Beavis, C. P. Roux, C. Weyermann and A. L. Gassner, *Forensic Sci. Int.*, 2017, **277**, 241–251.
12 S. Charles, N. Geusens and B. Nys, *Forensic Sci. Int.*, 2023, **6**, 100302.
13 S. Charles, N. Geusens, E. Vergalito and B. Nys, *Forensic Sci. Int.*, 2020, **2**, 416–428.
14 E1588, *Standard Practice for Gunshot Residue Analysis by Scanning Electron Microscopy/Energy Dispersive X-Ray Spectrometry*, ASTM International, DOI: **10.1520/E1588-20**.
15 C. Vander Pyl, W. Feeney, L. Arroyo and T. Trejos, *Forensic Chem.*, 2023, **33**, 100471.
16 W. Feeney, K. Menking-Hoggatt, C. Vander Pyl, C. E. Ott, S. Bell, L. Arroyo and T. Trejos, *Anal. Methods*, 2021, **13**, 3024–3039.
17 T. D. Ledergerber, W. Feeney, L. Arroyo and T. Trejos, *Anal. Methods*, 2023, **15**(36), 4744–4757.
18 C. Ott, K. Dalzell, P. Calderón-Arce, A. Alvarado-gamez, T. Trejos and L. Arroyo, *J. Forensic Sci.*, 2020, **65**(6), 1935–1944.
19 *Standard Practice for the Collection, Preservation, and Analysis of Organic Gunshot Residues*, OSAC, 2020, pp. , pp. 1–14.
20 S. R. Khandasammy, N. R. Bartlett, L. Halámková and I. K. Lednev, *Chemosensors*, 2023, **11**, 11.
21 D. N. Correa, J. M. Santos, L. S. Eberlin, M. N. Eberlin and S. F. Teunissen, *Anal. Chem.*, 2016, **88**, 2515–2526.
22 J. H. Gross, *Anal. Bioanal. Chem.*, 2014, **406**, 63–80.
23 M. J. Pavlovich, B. Musselman and A. B. Hall, *Mass Spectrom. Rev.*, 2018, **37**, 171–187.
24 R. Luten, D. Neimke, M. Barth and L. Niewoehner, *Forensic Chem.*, 2018, **8**, 72–81.
25 R. V. Gerard, M. J. McVicar, E. Lindsay, E. D. Randall and E. Harvey, *J.–Can. Soc. Forensic Sci.*, 2011, **44**, 97–104.
26 E. Lindsay, M. J. McVicar, R. V. Gerard, E. D. Randall and J. Pearson, *J.–Can. Soc. Forensic Sci.*, 2011, **44**, 89–96.
27 H. Mei, P. Han, Y. Wang, N. Zeng, D. Liu, Q. Cai, Z. Deng, Y. Wang, Y. Pan and X. Tang, *Sensors*, 2020, **20**, 1–17.
28 B. Alfano, L. Barretta, A. Del Giudice, S. De Vito, G. Di Francia, E. Esposito, F. Formisano, E. Massera, M. L. Miglietta and T. Polichetti, *Sensors*, 2020, **20**, 1–56.
29 M. Zusman, C. S. Schumacher, A. J. Gassett, E. W. Spalt, E. Austin, T. V. Larson, G. Carvlin, E. Seto, J. D. Kaufman and L. Sheppard, *Environ. Int.*, 2020, **134**, 105329.
30 H. Chojer, P. T. B. S. Branco, F. G. Martins, M. C. M. Alvim-Ferraz and S. I. V. Sousa, *Atmos. Environ.*, 2022, **286**, 119251.
31 Y. Zou, J. D. Clark and A. A. May, *Aerosol Sci. Technol.*, 2021, **55**, 848–858.

32 C. Vander Pyl, K. Dalzell, K. Menking-Hoggatt, T. Ledergerber, L. Arroyo and T. Trejos, *Forensic Chem.*, 2023, **34**, 100498.
33 S. Makhsous, J. M. Segovia, J. He, D. Chan, L. Lee, I. V. Novosselov and A. V. Mamishev, *Sensors*, 2021, **21**, 3298.
34 T. P. Forbes and M. Staymates, *Anal. Chim. Acta*, 2017, **957**, 20–28.
35 M. Staymates, G. Gillen, W. Smith, R. Lareau and R. Fletcher, in *ASME 2010 3rd Joint US-European Fluids Engineering Summer Meeting: Volume 2, Fora*, ASMEDC, 2010, pp. 203–209.
36 H. Ditrich, *Forensic Sci. Int.*, 2012, **220**, 85–90.